World Academy of Science, Engineering and Technology
International Journal of Structural and Construction Engineering
Vol:17, No:3, 2023

Monitoring and Analysis of Bridge Crossing Ground Fissures

Zhiqing Zhang, Xiangong Zhou, Zihan Zhou

***Abstract*—**Ground fissures can be seen in some cities all over the world. As a special urban geological disaster, ground fissures in Xi'an have caused great harm to infrastructure. Chang'an Road Interchange in Xi'an City is a bridge across ground fissures. The damage to Chang'an Road interchange is the most serious and typical. To study the influence of ground fissures on the bridge, we established a bridge monitoring system. The main monitoring items include elevation monitoring, structural displacement monitoring, etc. The monitoring results show that the typical failure is mainly reflected in the bridge deck damage caused by horizontal tension and vertical dislocation. For the construction of urban interchange spanning ground fissures, the interchange should be divided reasonably, a simple support structure with less restriction should be adopted, and the monitoring of supports should be strengthened to prevent the occurrence of beam falling.

***Keywords*—**Bridge monitoring, ground fissures, typical disease, structural displacement.

I. Introduction

AS a kind of geological disaster phenomenon, the ground fissure has attracted the attention of bridge academic circles. Some scholars have used existing monitoring technologies to observe and monitor this geo-hazard [1], [2].

Xi'an is one of the cities suffering from serious ground fissure disasters in China. Since the 1950s, more than 10 ground fissures have been found in Xi'an. Experts generally believe that the ground fissures in Xi'an city belong to the typical multiple cause superimposed ground fissures, which have the basic characteristics of structural ground fissures as well as the displacement superimposition of ground subsidence [3]-[6].

Peng et al. studied the ground fissures in Xi'an for years and regarded them as the most typical ground fractures in China [7]. 14 fissures have divided the city into several distinct parts. The fissures were generated under the coupling action of multiple factors [8]. Research shows that the ground fissures in Xi'an produce three-dimensional motion, among which the vertical displacement has the strongest effects on metro engineering [9]. The mechanism that failures of metro tunnels pass obliquely through ground fissures at low angles are also explored [10].

Zhang et al. assessed the effective stress in the design of underground engineering structures across a ground fissure zone, and a method to calculate the overlying load on the utility tunnel caused by ground fissure activity was proposed [11]. They discussed the deformation mechanism of a utility tunnel crossing active ground fissures in Xi'an as observed in a physical model test, and found that observations mark a notable departure from the previously published failure mode of metro tunnels under active ground fissures [12].

Li et al. studied the effect of intersection angle for utility tunnel when crossing ground fissures, and compared outcomes when the utility tunnel crosses ground fissures with different intersection angles through a numerical simulation method [13]. Fan et al. summarized the formation of ground fissures and found that variations in the dip angles and cross angles influence road deformation and cracking. Based on survey data, a numerical simulation method was conducted to analyze the impact of ground fissures on roads [14].

Xiong et al. investigated the distributing disciplinarian of ground motion parameters on the earth fissure site during strong earthquakes, a series of shaking table tests was designed and conducted based on 1:15 scaled models [15], [16]. The 3D finite element models containing the surface structure, underground station, and ground soil with earth fissure were built. Seismic behaviors of earth fissure ground were compared with the test result. The results indicate that the existence of earth fissures and surface structure amplifies the seismic responses of the underground station [17], [18].

Liu et al. conducted a shaking table model test and numerical simulation model on a scaled tunnel model to investigate the mechanism and effect of seismic loadings on the metro tunnel which is closely parallel to an active ground fissure [19], [20]. Results discovered the relationship between subsidence, widening of fissures, and the earthquake.

Zhang et al. [21] studied the influence of active ground fissures on the high-speed railway which has a small angle intersection with ground fissures. Pang et al. [22] discussed the bridge disaster mechanism under the influence of ground fissure activity simulated by a settlement platform. The results were compared with the ANSYS finite element.

The researches mainly focus on the impact of ground fissures on the utility tunnel, underground metro, and highway, with few studies on bridges. The working conditions and structural changes of these bridges are not clear for a long time. In order to study the influence of the ground fissure on the bridge structure, clarify the typical disease of this kind of bridge and its causes, and provide a reference for the construction and maintenance of bridges in other fissure active areas, our research group carried out a detailed investigation and monitoring on the Chang'an Road interchange and obtained some relevant results and conclusions.

Zhiqing Zhang is with Master of Engineering, Chang'an University, Xi'an China (corresponding author, e-mail: 2020121028@chd.edu.cn).

Xiangong Zhou is with Doctor of Engineering, Chang'an University, Xi'an China (e-mail: zhouxiangong@ chd.edu.cn).

Zihan Zhou is with Master of Engineering, Chang'an University, Xi'an China (e-mail: 2020221083@chd.edu.cn).

II. Engineering Background

A. Distributions of Ground Fissure in Xi'an

The distribution range of ground fissures in Xi'an is from Zaohe in the west to Fangzhicheng in the East, from Sanyao village in the south to Jingshang village in the north, covering an area of about 150 km^2. They are banded, quasi-parallel, and equidistant. The main ground fissures show the characteristic of a southward dip.

B. The Overview of Chang'an Road Interchange

Chang'an Road Interchange is located at the intersection of South 2nd Ring Road and Chang'an Road, which is a two-layer cloverleaf interchange. The upper structure of the north-south interchange bridge is simply supported prestressed hollow slab with a span of 10.2 m + 13.5 m + 13.5 m + 10.2 m. The total width of the bridge deck is 51.5 m (including railings). The upper layer of bridge deck pavement is 6 cm asphalt concrete, and the lower layer is 10 cm thick cast-in-place concrete. It was completed and opened to traffic in November 1994, see Figs. 1 and 2 for the appearance of Chang'an Road interchange.

Fig. 1 Outside view of Chang'an Road Interchange

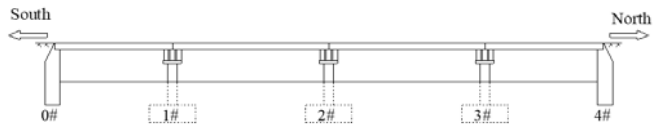

(a) Elevation of Chang'an Road Interchange

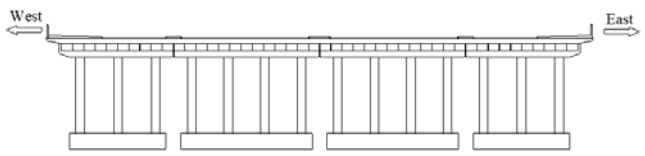

(b) Cross section of Chang'an Road Interchange

Fig. 2 Chang'an Road interchange schematic diagram

There is an F6 ground fissure under Chang'an Road Interchange; see Fig. 3 for the distribution of ground fissures around the bridge. The fissure has a long extension distance and a curved plane distribution. After crossing the interchange in the east, it extends along the direction of NE 55 ~ 65° and enters the Caochangpo village. There are obvious staggered deformations on the kerb near the interchange and the pier column under the bridge. From 1990 to 1999, the average activity rate of F6 ground fracture is 41 mm/a, and the maximum is 49.42 mm/a. The average activity rate from 2002 to 2005 is 3.1 mm/a. From the geological exploration results, there are obvious differences in the physical and mechanical properties of the rock and soil on both sides of the ground fracture: the water content on the north side of the ground fracture is 19.2%, and that in the south side is 26.1%. The compression coefficient of the north plate is 0.22 MPa^{-1}, that of the south plate is 0.35 MPa^{-1}, and the dry density is 14.9 kN/m^3. The shear strength C value has little difference, and the φ value is increased by about 10°.

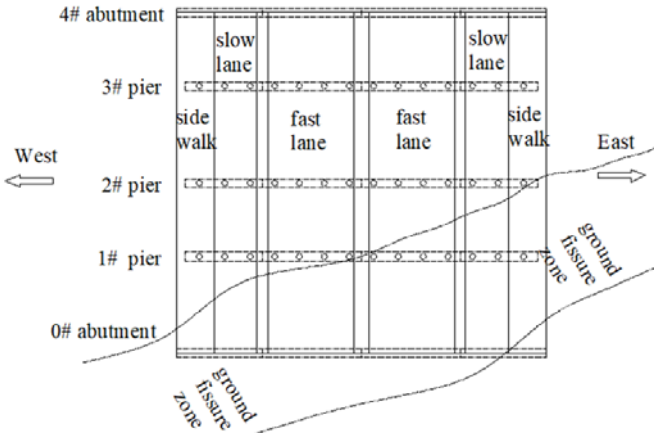

Fig. 3 Distribution of ground fissures around the bridge

III. Monitoring and Results

A. Deck Elevation

The permanent observation points in the northeast of the bridge, and the relative elevation is +0.000 m. Elevation measuring points are arranged on the bridge deck, at the position about 50 cm away from the expansion joint at the edge of each traffic lane. The arrangement and number of the elevation survey points of the two bridges in the west are symmetrical with the two bridges in the east, see Fig. 4 for the layout of bridge deck elevation survey points.

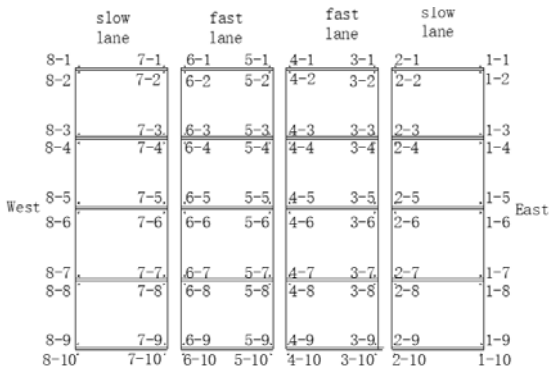

Fig. 4 Map of bridge deck elevation measuring point

Through the elevation measurement of these measuring points, we can observe the dislocation of the bridge deck and the common settlement accompanying the foundation. The measured results (from December 2020 to November 2021) are shown in Table I.

TABLE I
CUMULATIVE CHANGE VALUE OF BRIDGE DECK ELEVATION MEASURING POINT (UNIT: CM)

	8	7	6	5	4	3	2	1
1	0.3	0.6	0.6	0.5	0.4	0.3	0.3	0.3
2	0.4	0.4	0.6	0.5	0.4	0.3	0.3	0.3
3	0.1	0.1	0.6	0.5	0.3	0.3	0.4	0.0
4	-0.1	0.1	0.5	0.5	0.4	0.4	0.4	0.0
5	-0.1	0.0	0.3	0.3	0.3	0.3	0.0	0.2
6	-0.1	-0.1	0.2	0.3	0.2	0.3	0.1	0.2
7	-0.3	-0.1	-0.4	-0.2	0.0	0.2	0.2	0.3
8	-0.3	-0.3	-0.4	-0.2	-0.1	0.2	0.1	0.3
9	-0.3	0.1	-0.2	-0.1	-0.2	0.3	0.3	0.5
10	-0.2	0.2	-0.3	-0.2	-0.2	0.4	0.2	0.4

According to Table I, during the monitoring period, the elevation of the bridge deck at the northwest side has an overall upward trend, with an upward range of 1-6 mm. The elevation of the bridge deck at the southeast side of the ground fissure also has a rising trend, with a rise of 1-5 mm. In the ground fissure area, the southwest corner of the bridge deck is in a state of decline, with a maximum decline of 4 mm. The deck in the northeast corner rises a little.

B. Piers and Abutments Elevation

Through the comparison and analysis of the data obtained from the regular elevation survey of piers and abutments, the change of elevation can be judged. The measurement frequency is once every two months. The layout plan of abutment and pier measuring points is shown in Fig. 5.

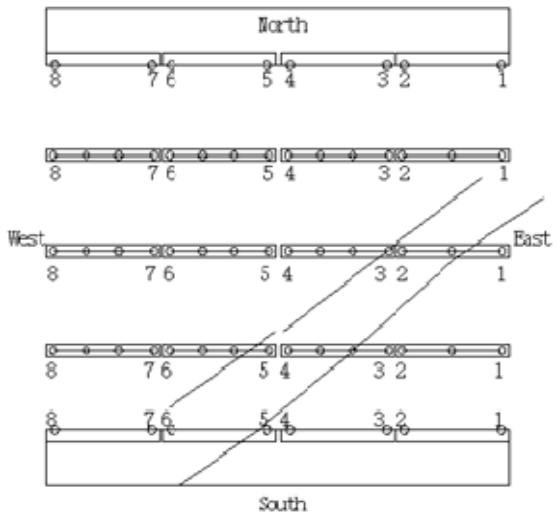

Fig. 5 Abutment and pier elevation monitoring

The data of the using state of the bridge substructure are obtained. The accumulated change value (from December 2020 to November 2021) of pier (abutment) measuring points is given in Table II. According to Table II, during the monitoring period, the change rule of the pier's elevation is that the pier (abutment) in the southwest corner is in a descending state. The maximum decline range is 4.5 mm (the maximum change value is at No. 6 measuring point of 1# pier). The pier in the northeast corner rises a little. Outside the ground fissure area, the pier (abutment) is in the rising state, and the maximum rising range is up to 7.5 mm.

TABLE II
ACCUMULATED CHANGE VALUE OF PIER (ABUTMENT) MEASURING POINT (UNIT: CM)

Point / Piers	Point 8	Point 7	Point 6	Point 5	Point 4	Point 3	Point 2	Point 1
4#	0.55	0.75	0.65	0.65	0.55	0.40	0.35	0.35
3#	0.20	0.65	0.70	0.65	0.45	0.40	0.40	0.05
2#	-0.05	0.20	0.20	0.35	0.25	0.35	0.10	0.25
1#	-0.40	-0.30	-0.45	-0.15	-0.05	0.20	0.20	0.30
0#	-0.35	-0.30	-0.30	-0.15	-0.25	0.40	0.25	0.50

C. Bridge Deck Expansion Joint Width

Due to the influence of ground fissures and uneven settlement, the pier and abutment settlement of Chang'an Road Interchange is staggered. This causes the bearing void, displacement, and inclination of the beam structure. These typical diseases reflect in the vertical dislocation, the horizontal tension, and extrusion of the expansion joint. Part of the expansion joint is squeezed, which loses the deformation function of the expansion joint and affects the working state of the bridge. To further understand the deformation trend of the expansion joint, we measure and analyzed the expansion joint width once a month. We use the measurement of the distance of the cross screw on both sides of the expansion joint to monitor the width change of the expansion joint (Fig. 6).

Fig. 6 Measuring point of expansion joint width

There are five expansion joints in the whole bridge, eight distances are measured for each expansion joint. To make the measurement results accurate and comparable, the width measurement is carried out regularly with fixed measurement points, fixed measurement personnel, and fixed measurement tools. Expansion joints are numbered in sequence from south to north, each expansion joint is measured eight intervals from east to west. The accumulated change value (from December 2020 to November 2021) of measuring points is given in Table

III.

TABLE III
THE ACCUMULATED CHANGE VALUE OF MEASURING POINT (UNIT: CM)

Expansion joint	1	2	3	4	5	6	7	8
First	0.4	0.2	0.1	0.2	-0.2	0.3	0.2	0.4
Second	0.1	0.2	0.2	0.1	0.3	0.4	0.1	0.2
Third	-0.2	-0.4	0	-0.2	-0.3	-0.1	0	0.1
Fourth	-0.3	-0.2	-0.4	-0.3	0	0.1	-0.2	-0.4
Fifth	-0.5	-0.4	-0.4	-0.4	-0.3	-0.1	-0.3	-0.4

According to Table III, the width of the first and second expansion joints from south to north tends to increase, with a maximum cumulative increase of 4 mm. The width of the third, the fourth, and the fifth expansion joints tends to decrease, with a maximum cumulative decrease of 5 mm.

D.Height Difference Monitoring of Capping Beam

The second and third bridges built on 1# pier from the east are located in the ground fissures, and the height difference is greatly affected by the ground fissures as shown in Fig. 7. The observation point is the end of the cap beam on No. 7 and No. 8 columns of 1# pier. As a key monitoring object, the height difference of the capping beam is measured once a month. The layout plan of abutment and pier measuring points is shown in Fig. 5.

Fig. 7 Height difference of capping beam

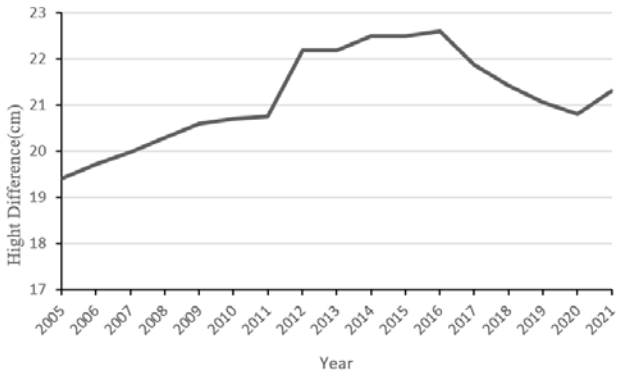

Fig. 8 Change of relative height difference of capping beam over years (cm)

The changing trend of the relative height difference between the West 2 and the West 3 capping beams of 1# pier over the years (from 2005 to 2021) is shown in Fig. 8. According to Fig. 8, the relative height difference of the capping beam tends to be smaller after 2016. At the end of the monitoring period (November 2021), the height difference reached 21.3 cm, which was increased compared with 20.8 cm at the beginning of the monitoring period (December 2020). During the 2020-2021 monitoring period, the relative height difference of the capping beam has a growth trend of 5 mm, and it is stable at 21.3 cm in the last three months. In addition, according to the monitoring data of 2# pier, the distance between the East 1 and the East 2 capping beams is stable at 19.3 cm during the monitoring period. It shows that the ground fissures increase but have little effect on the displacement of the piers in this observation period.

E. Bridge Bearing Condition

The upper structure of the Chang'an Road interchange is simply supported hollow slab. Because of the influence of ground fissure, the position with a larger expansion joint width may have the risk of beam falling. For the inspection of the bearing condition, it is necessary to combine the monitoring results of the expansion joint width in previous years to detect the relative overlapping position of the bearing and the hollow slab at the position with a large expansion joint. The measurement diagram is shown in Fig. 9.

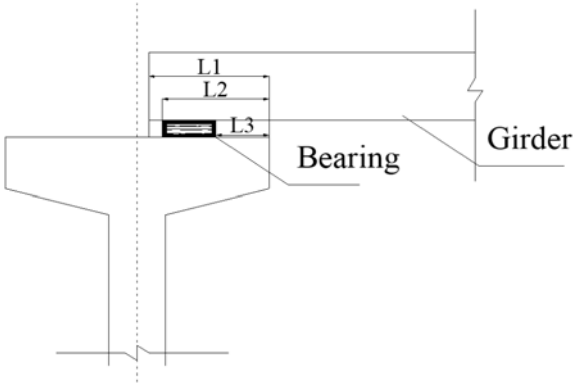

Fig. 9 Schematic diagram of bearing deflection measurement

From the measurement data (from December 2020 to November 2021), it can be concluded that most L1-L2 ≥ 5 cm, only six bearings L1-L2 < 5 cm, and the smallest is 1.0 cm. This is because the bearing is placed too close to the middle of the capping beam. Therefore, it can be seen that the cantilever length of the hollow slab on the upper part of the support is greater than 0, which has a certain amount of safety margin, and there is no risk of falling the beam under normal conditions. In addition, it is found that some bearings have obvious shear deformation in the process of monitoring.

F. Structural Dynamic Performance

The natural frequency of the bridge structure is related to the rigidity of the bridge structure, and the development of the crack at the bottom of the beam will cause a change in the

flexural rigidity of the reinforced concrete bridge. The monitoring of the bridges working state can be realized by detecting the dynamic performance of the bridge structure. The bridge span number is shown in Fig. 10. Using the dynamic signal and analysis system to monitor the free vibration frequency of the structure. The real-time speed signal and fundamental frequency were obtained.

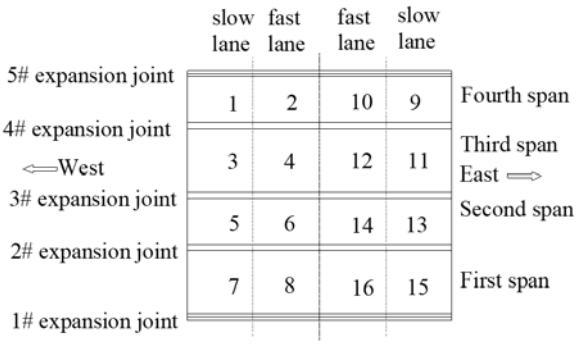

Fig. 10 Bridge span numbering

The first-order natural frequency was analyzed and calculated. The dynamic performance parameters of the structure are obtained and the parameters are compared with the theoretical values. The results are shown in Table IV, According to the table, the measured fundamental frequency is greater than the theoretical value, and the bridge is in good working condition. This is because bridge deck pavement, guardrail, and other components will increase the stiffness of the structure, and the stiffness contribution of these components is not considered in the calculation.

TABLE IV
MEASURED FUNDAMENTAL FREQUENCY OF EACH BRIDGE SPAN

Span number	First mode shape	
	Frequency measured (Hz)	Frequency calculated (Hz)
1	14.84	9.50
2	14.45	9.50
3	8.40	5.20
4	8.40	5.20
5	8.79	5.20
6	8.79	5.20
7	14.84	9.50
8	12.50	9.50

IV. CONCLUSIONS

1. The movement of ground fissures will lead to the relative displacement or corner of each span beam. These geometric deformations are digested by the bridge separation zone on the bridge deck and do not cause large stress damage to the structure.
2. For the construction of the bridge across ground fissures, it is necessary to adopt simple support structure with less constraint and divide the interchange into reasonable blocks to reduce the harm of ground fissures to urban interchange. Generally, the main measure is to strengthen the monitoring to prevent the serious consequences of beam falling.
3. Through reasonable monitoring, the actual working condition of the bridge can be obtained, and provide a strong basis for the bridge management and maintenance work.

ACKNOWLEDGMENT

This work was financially supported by Nature Science Basic Research Program of Shaanxi, China. (Program No. 2020JQ-377).

REFERENCES

[1] Wang Zhi-feng, Cheng Wen-chieh, and Wang Ya-qiong. Investigation into Geohazards During Urbanization Process of Xi'an, China. (J) Natural Hazards 92, no. 3 Jul 2018: 1937-53. http://dx.doi.org/10.1007/s11069-018-3280-5

[2] Wang, Bao-hang, Zhao Chao-ying, et al. Sequential Insar Time Series Deformation Monitoring of Land Subsidence and Rebound in Xi'an, China. (J) Remote Sensing 11, no. 23 Dec 2019: 17. http://dx.doi.org/10.3390/rs11232854.

[3] Peng, Mi-mi, Zhao Chao-ying, Zhang Qin, LU Zhong, and LI Zhong-sheng. Research on Spatiotemporal Land Deformation 2012-2018 over Xi'an, China, with Multi-Sensor Sar Datasets. (J) Remote Sensing 11, no. 6 Mar 2019: 21. http://dx.doi.org/10.3390/rs11060664.

[4] Liu Xi, Ma Jing, and Su Shan. Factors Influencing Activity of Xiwang Road Ground Fissure Based on Time-Series Interferometric Synthetic Aperture Radar and Detection of Land Cover Changes Using Optical Imaging. (J) Sensors and Materials 32, no. 12 2020: 4635-46.

[5] Wang, Fei-yong, Peng Jian-bing, Lu Quan-zhong, Cheng Yu-xiang, Meng Zhen-jiang, and Qiao Jian-wei. Mechanism of Fuping Ground Fissure in the Weihe Basin of Northwest China: Fault and Rainfall. (J) Environmental Earth Sciences 78, no. 14 Jul 2019: 10. http://dx.doi.org/10.1007/s12665-019-8421-y

[6] Peng Jian-bing, Qiao Jianwei, Leng Yan-qiu, Wang Fei-yong, and Xue. Shou-zhong. Distribution and Mechanism of the Ground Fissures in Wei River Basin, the Origin of the Silk Road. (J) Environmental Earth Sciences 75, no. 8 Apr 2016: 12. http://dx.doi.org/10.1007/s12665-016-5527-3.

[7] Peng Jian-bing, Wang Fei-yong, Cheng Yu-xiang, and Lu Quan-zhong. Characteristics and Mechanism of Sanyuan Ground Fissures in the Weihe Basin, China. (J) Engineering Geology 247 Dec 2018: 48-57. http://dx.doi.org/10.1016/j.enggeo.2018.10.024.

[8] Peng Jian-bing, Qu Wei, Ren Jun, Zhang Qin, and Wang Fei-yong. Geological Factors for the Formation of Xi'an Ground Fractures. (J) Journal of Earth Science 29, no. 2 Apr 2018: 468-78. http://dx.doi.org/10.1007/s12583-018-0841-1.

[9] Peng Jian-bing, Huang Qiang-bing, Hu Zhi-ping, Wang Ming-xiao, Li Tan, Men Yu-ming, and Fan Wen. A Proposed Solution to the Ground Fissure Encountered in Urban Metro Construction in Xi'an, China. (J) Tunnelling and Underground Space Technology 61 Jan 2017: 12-25. http://dx.doi.org/10.1016/j.tust.2016.09.002.

[10] Peng Jian-bing, He Kai, Tong Xiao, Huang Qiang-bing, and LIU Chong. Failure Mechanism of an Underground Metro Tunnel Intersecting Steep Ground Fissure at Low Angle. (J) International Journal of Geomechanics 17, no. 5 May 2017: 13. http://dx.doi.org/10.1061/ascegm.1943-5622.0000677

[11] Zhang Dan, Hu Zhi-ping, Lu Gang-gang, Wang Rui, and Ren Xiang. Calculation of the Vertical Strata Load of Utility Tunnel Crossing Ground Fissure Zone. (J) Shock and Vibration 2020 Dec 2020: 12. http://dx.doi.org/10.1155/2020/8877016.

[12] Zhang Dan, Hu Zhi-ping, Lu Gang-gang, Wang Rui, and Ren Xiang. Experimental Study on Deformation Mechanism of a Utility Tunnel in a Ground Fissure Area. (J) Advances in Materials Science and Engineering 2020 May 2020: 15. http://dx.doi.org/10.1155/2020/6758978.

[13] Li Fang-tao, Wang Qi-yao, Hu Zhi-ping, Zhang Yong-hui, Ren Xiang, and An. Xue-xu. The Effect of Intersection Angle on the Failure Mechanism of Utility Tunnel. (J) Advances in Civil Engineering 2020 Nov 2020: 16. http://dx.doi.org/10.1155/2020/8864676.

[14] Fan Wen, Peng Xiang-lin, Deng Long-sheng, and Jiang Cheng-cheng.

The Study of Road Deformation Induced by Ground Fissure in Xi'an, Central China. (J) Arabian Journal of Geosciences 13, no. 15 Jul 2020: 12. http://dx.doi.org/10.1007/s12517-020-05716-w.

[15] Xiong Zhong-ming, Zhang Chao, Huo Xiaopeng, Chen Xuan, and Ochoa, J. Jorge. Distributing Disciplinarian of Ground Motion Parameters on an Earth Fissure Site During Strong Earthquakes. (J) Earthquake Engineering and Engineering Vibration 19, no. 3 Jul 2020: 597-610. http://dx.doi.org/10.1007/s11803-020-0583-9.

[16] Xiong, Zhong-ming, Chen Xuan, Zhang Chao, Huo Xiao-peng, and Zhuge, Yan. Shaking Table Tests of Rc Frame Structure across the Earth Fissure under Earthquake. (J) Structural Design of Tall and Special Buildings 27, no. 14 Oct 2018: 15. http://dx.doi.org/10.1002/tal.1496

[17] Xiong, Zhong-ming, Chen Xuan, Wang Yong-wei, Xiong Weiyang, and Ochoa, J. Jorge. Dynamic Performance of Rc Structure Crossing Ground Fissure. (J) Journal of Structural Engineering 146, no. 5 May 2020: 15. http://dx.doi.org/10.1061/ascest.1943-541x.0002624.

[18] Xiong, Zhong-ming, Wang Yong-wei, Chen Xuan, and Xiong Wei-yang. Seismic Behavior of Underground Station and Surface Building Interaction System in Earth Fissure Environment. (J) Tunnelling and Underground Space Technology 110 Apr 2021: 14. http://dx.doi.org/10.1016/j.tust.2020.103778.

[19] Liu Ni-na., Lu, Quan-zhong, Feng Xiao-yang, Fan Wen, Peng, Jian-bing, Liu Weiliang, and Kang Xin. Dynamic Characteristics of Metro Tunnel Closely Parallel to a Ground Fissure. (J) Complexity 2019: 11. http://dx.doi.org/10.1155/2019/6450853.

[20] Liu Ni-na, Huang Qiangbing, Wang Li, Fan Wen, Jiang Zikan, and Peng Jianbing. Dynamic Characteristics Research of a Ground Fissure Site at Xi'an, China. (J) Tunnelling and Underground Space Technology 82 Dec 2018: 182-90. http://dx.doi.org/10.1016/j.tust.2018.08.044.

[21] Zhang Yin-tao, Zhang Chen, Huang Qiang-bing. Study on the damage mechanism of ground crack to high-speed railway bridge. (J) Railway Engineering: 06 2014: 24-26. 10.3969 /j. issn, 1003-1995．2014．06．07 (In Chinese)

[22] Pang Xv-qing, Liu Hong-jia, Yan Jing-ping. Test and research on mechanism of bridge disaster under ground fissure. (J) High Way: 6205 2017:70-75 doi:CNKI:SUN:GLGL.0.2017-05-015. (In Chinese)